

Cellular compartment specific T₂* relaxation in white matter

Pascal Sati¹, Peter van Gelderen², Afonso C Silva³, Daniel S Reich¹, Hellmut Merkle⁴, Jacco A De Zwart², and Jeff H Duyn²

¹Translational Neuroradiology Unit, Neuroimmunology Branch, National Institute of Neurological Disorders and Stroke, Bethesda, Maryland, United States,

²Advanced MRI Section, Laboratory of Functional and Molecular Imaging, National Institute of Neurological Disorders and Stroke, Bethesda, Maryland, United States, ³Cerebral Microcirculation Unit, Laboratory of Functional and Molecular Imaging, National Institute of Neurological Disorders and Stroke, Bethesda, Maryland, United States, ⁴Laboratory of Functional and Molecular Imaging, National Institute of Neurological Disorders and Stroke, Bethesda, Maryland, United States

Target Audience: Clinicians and basic scientists studying the brain

Purpose: At high field, brain tissues show complex T₂* relaxation characteristics that provide unique contrast but are not fully understood. Specifically, recent work has shown multi-component relaxation in white matter that is orientation dependent [1], which may be caused by the magnetic properties of myelin. Here we performed measurements, multi-component fitting, and simulations to investigate whether the cellular and molecular structure of myelin may explain these observations, and whether the individual relaxation components can be assigned to distinct cellular compartments.

Methods: T₂* relaxation was investigated with multi-gradient echo acquisition (MGRE) MRI in four healthy volunteers and four healthy marmoset monkeys on 7T animal and human scanners. Because marmosets are more amenable to head rotation in the bore of an MRI system [2], and their brain has a relatively straightforward white matter (WM) fiber geometry, one marmoset was also used for investigating the orientation dependence of T₂* relaxation. Magnetic field simulations were performed using a Fourier based method at the micron and millimeter scales to investigate the effect of myelin on compartment-specific relaxation and contrast in phase and magnitude images. A three-compartment model of myelinated, cylindrical axons of non-uniform size was used at various angles with the field. These simulations also included anisotropic diamagnetic susceptibility for the myelin sheath [3,4], and field averaging effects from water diffusion. For the macroscopic (millimeter scale) simulation, brain geometry and fiber angle were derived from DTI measurements. Complex signal decay both averaged over different WM fibers ROIs, as well as on a pixel-by-pixel basis, was fitted modeling multiple decay rates and frequencies. To improve robustness of the pixel-by-pixel fit, a nested model was used involving successively a one-component fit, then a two-components fit, and finally a three-component fit.

Results: Signal evolution with echo time in WM fibers of marmosets and humans was found to be complicated suggesting the presence of three major signal components C1-C3 with different values of R₂* signal decay and frequency shift Δf (Table 1 and Fig. 1). This multi-component relaxation was also highly dependent on the orientation of the fibers relative to the main B₀ field (Table 1 and Fig. 1). Component 1 (C1) with the highest R₂* value was attributed to myelin water, whereas C2 and C3 were tentatively attributed to interstitial and axonal water, respectively. Although these two components have similar amplitudes and R₂* values, their frequency shift values are sufficiently different, making them distinguishable. The effect of fiber orientation on R₂* and Δf as a function of echo time measured in the optic radiations of the marmoset can also be explained by the simulations of magnetic field effects associated with anisotropic susceptibility of the myelin sheath (Fig 2), consistent with [5]. These simulations also confirmed the assignment of interstitial and axonal water to C2 and C3.

Conclusions: At high field, the study of R₂* signal decay in combination with frequency shift Δf may allow the identification of myelin water, and the distinction between axonal and interstitial water. These findings would be valuable for the study of demyelinating diseases such as multiple sclerosis (MS).

References: [1] Van Gelderen et al., MagnReson Med 67 (1):110-117; [2] Sati et al., Neuroimage 59 (2):979-985; [3] Lee et al., Neuroimage 57(1):225-234; [4] Li et al., Neuroimage 59(3):2088-2097; [5] Wharton and Rowlett PNAS Early Ed (2012)

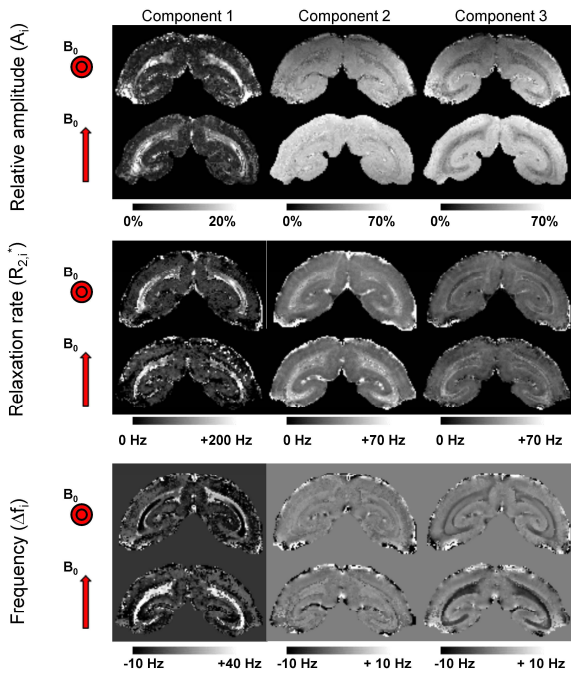


Figure 1: Multi-component orientation-dependent MRI relaxation in marmoset brain. Components 1, 2 and 3 are attributed to myelin water, interstitial water and axonal water, respectively.

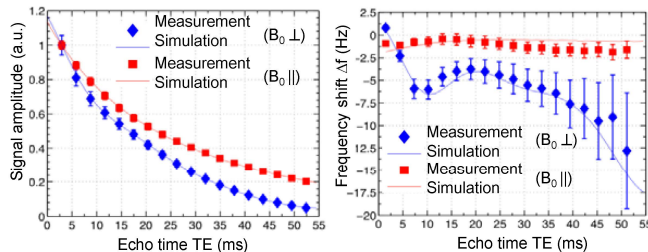


Figure 2: T₂* signal decay and frequency shift measured in the optic radiations of the marmoset at 7T.

Table 1: Results of the curve fitting for the optic radiations in marmoset and human brains (n = number of animals / human subjects). A_i , $R_{2,i}^*$, and Δf_i correspond to the relative amplitude, relaxation rate, and frequency shift of the individual components, respectively. Values are the mean (standard deviation) calculated across the four animals or four human subjects.

	n	B_0	A_1 , %	$R_{2,1}^*$, Hz	Δf_1 , Hz	A_2 , %	$R_{2,2}^*$, Hz	Δf_2 , Hz	A_3 , %	$R_{2,3}^*$, Hz	Δf_3 , Hz
Human	4	⊥	19.0 (1.5)	165.1 (10.7)	25.1 (1.8)	42.3 (1.6)	28.3 (2.9)	1.5 (0.3)	38.7 (1.0)	27. (2.0)	-6.0 (0.6)
Marmoset	4	⊥	20.2 (1.5)	186.4 (25.7)	25.7 (3.1)	32.7 (3.0)	32.1 (2.9)	2.5 (0.3)	47.1 (2.2)	30.6 (4.5)	-6.3 (0.5)
	1		21.3	134.8	-5.4	30.9	16.1	-2.5	47.9	34.7	1.1